

## Analysis of Deformation of Segmental Lining during Shield Tunneling Based on Real-Time Monitoring

Jiaqi Chang<sup>1</sup>, Dongming Zhang<sup>2</sup>, Hongwei Huang<sup>3</sup>

<sup>1</sup>Key Laboratory of Geotechnical and Underground Engineering of Minister of Education and Department of Geotechnical Engineering, Tongji University, Shanghai, China.  
Email: cj1550750@163.com

<sup>2</sup>Key Laboratory of Geotechnical and Underground Engineering of Minister of Education and Department of Geotechnical Engineering, Tongji University, Shanghai, China.  
E-mail: 09zhang@tongji.edu.cn

<sup>3</sup>Key Laboratory of Geotechnical and Underground Engineering of Minister of Education and Department of Geotechnical Engineering, Tongji University, Shanghai, China.  
E-mail: huanghw@tongji.edu.cn

**Abstract:** The deformation of segmental lining is an important factor to evaluate the state of tunnel structure. In order to judge the mechanical condition of tunnel structure during construction, a wireless sensor network (WSN) is applied to monitor the tilt change and diameter convergence of 2 sections of a constructing Shanghai Metro tunnel. 4 tilt nodes and 1 distance laser nodes are installed on each section right after the erection to monitor the tilt change of standard segments, adjacent segments and the horizontal of the segmental rings with frequency of 10mins. When the segments are inside the shield tail, the laser nodes are blocked by the shield equipment and workers, unable to monitor the diameter. In order to get the diameter during this period, an ensemble machine learning method, gradient boosting method (GBR) is applied to calculate the diameter from the tilt angle. The monitored data of tilt and diameter reveal 2 deformation modes, the rotation and the ovalization, of the segmental linings during construction. The rotation is the main mode when the lining inside the shield tail and the maximum of rotation length is about 12mm. When the lining pulled out of shield tail, the ovalization becomes the main mode with about 2mm convergence of horizontal diameter happening in 1day. As the shield advanced, the horizontal diameter increases about 3mm in 6 months. The relationship between construction parameters and the deformations are analyzed. The cutter torque when shield advance is related to the rotation deformation. The tail grouting when the lining pulled out is related to the diameter convergence.

Keywords: shield tunnel; construction; wireless sensor network; segment deformation; tilt angle; diameter convergence

### 1 Introduction

Many methods have been used to monitor the deformation of shield tunnels since the deformation is important to evaluate the state of tunnel structure in all stages, including construction period and service period (Ariznavarreta-Fernandez et al., 2016). The deformation of tunnel is an intuitive factor to evaluate the tunnel structure since the joint opening, segment cracks and other tunnel defects are closely related to the deformation (Shi et al., 2016; Huang et al. 2017a).

Due to the importance of deformation monitoring, many methods have been applied. Recently, total station, three-dimensional laser scanning and digital close-range photogrammetry are popular methods to monitor the shield tunnel deformation. But the low monitoring frequency and demanding light quality limit the application of the methods (Huang et al., 2020; Li and Yuan, 2012; Wang, 2020a; Xu, 2019) in construction period.

Wireless sensor network (WSN) is a new monitoring method which applies sensor nodes monitoring the tilt change of segments and convergence of segment rings. The nodes are small and the monitoring frequency can be adjusted flexibly (Huang et al., 2020b; Bennett et al., 2010a; Yin and Huang, 2015; Zhao et al., 2021; Wang et al., 2021a) invited a multisource information fusion monitoring system to guide the accurate construction and dynamic adjustment of support structure.

The studies of WSN application in tunnel engineering show that WSN has quick installation, little disturbance, strong adaptability and high frequency features and has been successfully adopted to monitor the long-term convergence variation of the shield tunnel in operation (Huang et al., 2017b). However, quite few reports have been published for the application of WSN system on the monitoring of shield tunnel lining at the construction stage because the construction machine will affect the signal transportation.

Considering the above situations, a case study of applying WSN to monitoring the shield tunnel deformation during construction period is presented in this paper. The construction period starts from the erection of the segmental lining and ends at the beginning of operation period. The processes of pushing jacks

loading on, segment linings coming out of shield tail, grouting pressure loading on and soil pressure loading on are all included so that the monitoring result is helpful to understand the deformational behavior of the tunnel linings.

## 2 Site Information

### 2.1 Geological profile

The installation project of this paper is a constructing metro line in Shanghai, passing through an operational metro line tunnel with distance of about 1.5m. The depth of overburden is from 20m to 25m. The new constructing tunnel passes through 3 stratum including ⑤1-2 grey silt clay, ⑥ dark green silt clay and ⑦1-2 grass yellow ~ grey yellow silt sand. The longitudinal profile is shown in Figure 1 and the properties of stratum is shown in Table 1.

### 2.2 Tunnel structure

The tunnel section is typical metro section in Shanghai with the out diameter of 6.6m and the thickness of 0.35m as shown in Figure 2. The longitudinal width of one ring is 1.2m and the segments are erected under straight joint assembling. There are 6 segments in one ring: 1 bottom segment (D), 2 standard segments (B1, B2), 2 adjacent segments (L1, L2) and 1 key segment (F). 2 steel bolts are fixed at each longitudinal joints and 17 steel bolts are fixed at each circumferential joints. The bolts are straight bolts with diameter of 30mm and the diameter of bolt holes is 33mm.

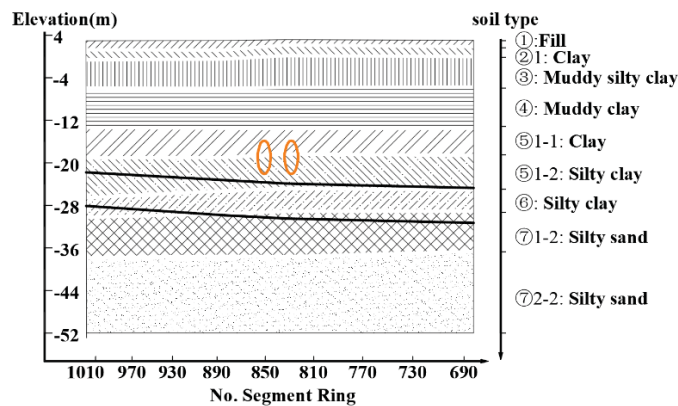


Figure 1. Longitudinal profile

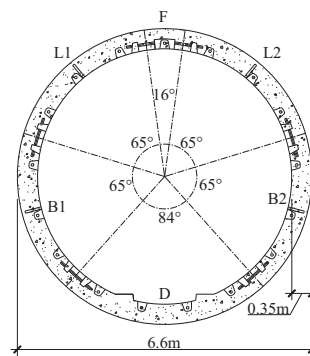


Figure 2. Cross section of segment ring

Table 1. Stratum properties

Soil type	Water content (%)	Density (kN/m <sup>3</sup> )	$k_0$	CQD cohesion (kPa)	CQD internal friction angle (kPa)	Specific penetration resistance (MPa)
②1	31.3	18.2	0.49	22	15	0.54
③	31.6	17.3	0.50	12	15	0.48
④	47.3	16.7	0.56	14	11	0.63
⑤1-1	37.9	17.7	0.51	17	12	0.95
⑤1-2	35.5	17.9	0.46	18	18	1.39
⑥	24.9	19.6	0.46	46	16	2.86
⑦1-2	25.5	19.1	0.39	4	32	10.88

### 3 Wireless Sensor Network

#### 3.1 Installation of WSN

The nodes installed on the Ring No. 831 and Ring No. 833 sections. The installed location of tilt angle is  $45^\circ$  and  $120^\circ$  from the center of key segment and that of laser nodes is  $90^\circ$ . The installation profile is shown in Figure 3 where UR means the upper-right tilt nodes, UL means the upper-left tilt nodes, DR means the down-right tilt nodes and DL means the down-left tilt nodes. The nodes are installed right after the erection of the segment ring and before the advance of the next ring so the monitoring data can reflect the structure deformation under the construction load. The nodes are fixed with the screws in the C shape groove and the installation of 1 node cost about 5min.

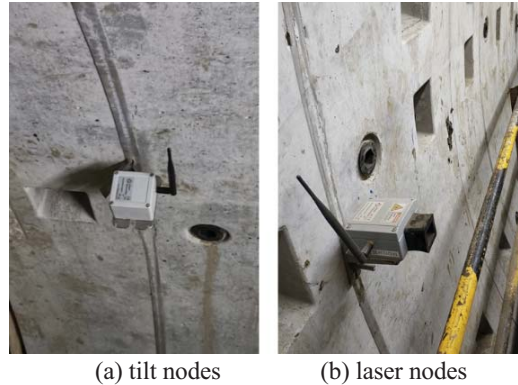


Figure 3. Installed nodes in site

### 4 Segment Deformation in Construction Period

#### 4.1 Data treatment

The monitor results from tilt nodes and laser nodes on Ring No. 831 are shown in Figure 4. The positive direction of the tilt is clockwise. The tilt data shows that the in the first 2 days after installation, the tilt change frequently and after the shield machine advance away, DR and UL increase, UR and DL decrease, showing a horizontal ovalization deformation with the horizontal diameter increasing which matches the laser data as shown in Fig. 5. The laser nodes in the first 23days after installation are blocked up by the workers and back-up trains frequently, causing the monitoring data full of noise and unable to use. Since the diameter change is important to judge the structure state, the diameter change in the first 23days needs to be calculated.

Some researchers (Wang, 2020) present a method to calculate the change of horizontal diameter with the tilt of segment:

$$\Delta D = L \cdot (\Delta\theta_1 - \Delta\theta_2) \cdot \cos\alpha \quad (1)$$

where  $\Delta D$  means the change of diameter,  $L$  means the distance between the tilt node to the joint as shown in Figure 4,  $\Delta\theta_1$  means the tilt change of DL,  $\Delta\theta_2$  means the tilt change of DR,  $\alpha$  means the angle between horizontal to the line connecting tunnel center and DL or DR as shown in Figure 4. Using the method to calculate the horizontal diameter and compare the results with the monitoring data from laser node as shown in Figure 5. The results show that due to the complex load condition in construction period, formula (1) is not suitable to calculate the change of horizontal diameter.

In order to get the change of diameter during construction, a machine learning method, gradient boosting regression (GBR), is used to calculate the diameter change based on the monitoring data from tilt nodes. The gradient boosting regression method is a supervised learning method. The monitoring data of tilt nodes after the first 23 days are input data while the monitoring data of laser nodes after the first 23 days are label data. The dataset contains 20,843 pairwise data points. Each pairwise data point includes 4 tilt monitoring data and 1 distance laser monitoring data. 80% of the total of pairwise data points (i.e.,  $20,843 \times 0.8 = 16,674$ ) are used for the training and 20% of the total of pairwise data points (i.e.,  $20,843 \times 0.2 = 4,169$ ) are used for the testing. In testing set, the goodness-of-fit between the calculated values and the monitoring values are 0.89 for ring 831, 0.83 for ring 833 and the testing results are the black points shown in Figure 6. The results show that the calculating results is close to the monitoring dat. Thus, the GBR model established here can be used to calculate the diameter in the first 23days.

Using the GBR model to calculate the diameter during construction and the results are shown as the green line in Figure 6 compared with the black line, the monitoring data from distance laser nodes. The calculating

results show that for one segment ring, the construction period can be divided into 2 stages: 1) when the shield machine is close to the segment ring, under the load from construction, the segment rings' diameters first increase for around 1mm because of the dead load and then decrease for around 3mm because of the grouting load; 2) when the shield machine advances far from the ring, the dead loads of the segments and pressure from soil become the major load and the ring diameters increase for around 2mm. During the whole construction period, the segment rings experience reciprocating loads.

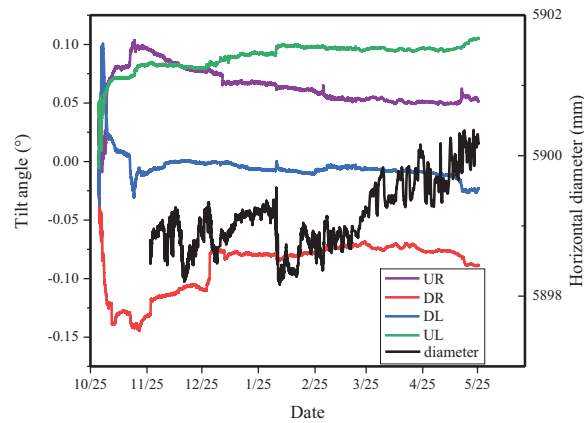


Figure 4. Monitoring data from nodes

Calculating the converge speed of diameter, the maximal speed of convergence is 19.4mm/d for ring 831 when constructing ring 833, from 10/29 19:08 to 10/29 19:28. The maximal speed of convergence is 23.9mm/d for ring 833 when constructing ring 840, from 10/31 19:48 to 10/31 20:18. The maximal convergence speeds are fast. Thus, the mechanical state of tunnel structure during construction period is complex and dangerous.

#### 4.2 Correlation analysis of monitoring data

The deformation under the load of construction is focused so the tilt data when the shield machine is not far from the monitoring ring is extracted and the abscissa is changed into the distance shield advances after installation as shown in Figure 7. Analyzing the tilt data, it can be found that before 3300mm, data from UR, UL, DR and DL have the same trend, i.e., have positive correlation coefficient with each other. This regular shows that before shield advances 3300mm, when the segmental ring is inside the shield tail, the deformation of segmental ring is whole rotation, i.e., UR, UL, DR and DL tilt clockwise or anti-clockwise together. After the segmental ring pulled out of shield tail, the nodes along the diagonal, i.e. UL and DR, UR and DL, show the same trend and the adjacent nodes show contrary trend. For example, UR tilts clockwise, DR tilts anti-clockwise, UL tilts anti-clockwise and DL tilts clockwise. This regular shows an ovalization deformation as shown in Figure 7.

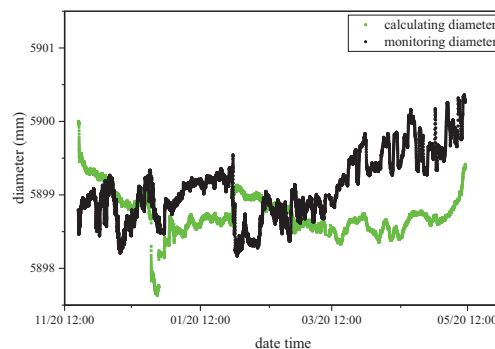


Figure 5. The calculating diameter with formula (1) and the monitoring diameter

The whole rotation is caused by the cutter rotation during advance. When the shield advance, the cutter rotates to cut the soil and the counterforce, i.e., the torque with negative direction of cutter loads on the shield. The friction between the pushing jacks of shield and the erected segments is to balance the torque, leading to the whole rotation of segments. The dead loads of segments cause the vertical diameter of segment ring to shorten and the horizontal diameter to lengthen, showing a horizontal ovalization deformation. Then the segment ring coming out of the shield tail, the pressures of tail grouting round the segment ring. At this moment, the segments

already have horizontal ovalization deformation so the rounding load make the horizontal diameter of ring shorten and the vertical diameter of ring lengthen, showing the vertical ovalization deformation.

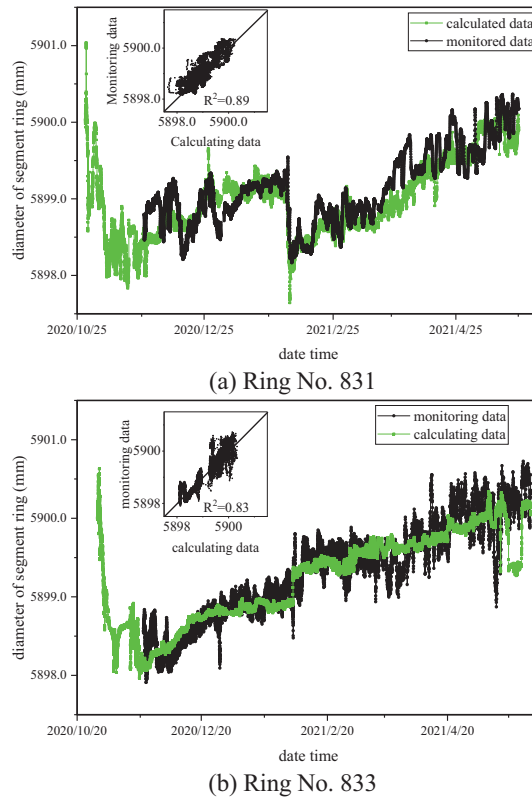


Figure 6. The calculating diameter with GBR and the monitoring diameter

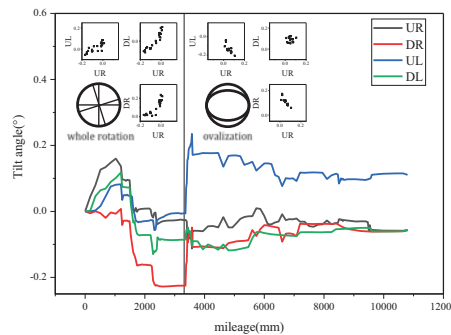


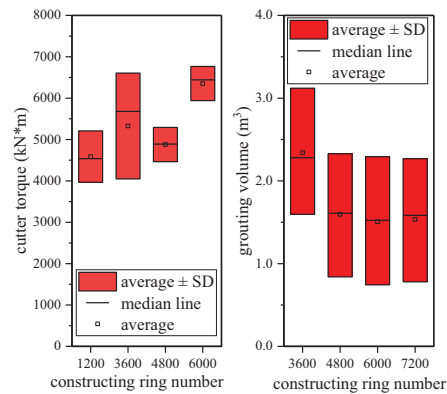
Figure 7. Monitoring data, correlation analysis and the deformation mode

### 5 Correlation of Construction Parameter

The shield machine contains 1008 construction parameters including cutter torque, force and stroke of pushing jacks, grouting volume and other parameters. Some of the construction parameters are shown in Figure 8. The monitoring sections are Ring No. 831 and Ring No. 833. The construction of the rings after the 2 rings will influence the deformation of these 2 rings. For example, Ring No. 831 is influenced by the cutter torque during constructing Ring No. 832, Ring No. 833 and the volume of grouting during constructing Ring No.834 and Ring No. 835. Similarly, Ring No. 833 is influenced by the cutter torque during constructing Ring No. 834, Ring No. 835 and the volume of grouting during constructing Ring No. 836 and Ring No. 837. In other words, in Figure 8, the left 2 boxes are the parameters influencing Ring No. 831 and the right 2 boxes or diamonds are the parameters mainly influencing Ring No. 833.

The cutter torques constructing Ring No. 834, 835 are larger than that of Ring No. 832, 833, meaning that Ring No. 833 suffers larger torque than Ring No. 831. For volume of grouting, the reverse applies. The different construction parameters might lead to different deformation values of Ring No. 831 and Ring No. 833. In Figure 6, the ovalization deformation of Ring No. 831 is 3mm, bigger than that of Ring No. 833 of 2.5mm. In Fig. 5, the

final whole rotation of Ring No. 831 is  $0.25^\circ$ , smaller than  $0.26^\circ$  of Ring No. 833. This reflects that the deformation of segmental lining is related to the value of construction parameters.



(a) cutter torque (b) grouting volume  
**Figure 8.** Values of construction parameters

## 6 Conclusion

A WSN system is applied in this paper to monitor the deformation of lining during tunnel construction. GBR technology is introduced to calculate the horizontal diameter based on the tilt data. The monitoring and calculating results show that the deformation of segmental lining during construction should not be ignored. There are two deformation mode during construction: whole rotation and ovalization. The value of the deformation is large and the speed is high compared to that during operation period. Construction parameters will influence the deformation so the parameters should be set properly to avoid the damage of lining.

## References

- Ariznavarreta-Fernandez, F., Gonzalez-Palacio, C., Menendez-Diaz, A., Ordonez, C. (2016). Measurement system with angular encoders for continuous monitoring of tunnel convergence. *Tunn. Undergr. Space Technol.* 56, 176-185.
- Shi, C.H., Cao, C.Y., Lei, M.F., Peng, L.M., Ai, H.J. (2016). Effects of lateral unloading on the mechanical and deformation performance of shield tunnel segment joints. *Tunn. Undergr. Space Technol.* 51, 175-188.
- Huang, H.W., Xiao, L., Zhang, D.M., Zhang, J. (2017). Influence of spatial variability of soil Young's modulus on tunnel convergence in soft soils. *Engineering Geology* 228, 357-370.
- Wang, F., Shi, J., Huang, H., Zhang, D., Liu, D. (2020). A horizontal convergence monitoring method based on wireless tilt sensors for shield tunnels with straight joints. *Structure and Infrastructure Engineering*, 1-16.
- Huang, H., Cheng, W., Zhou, M., Chen, J., Zhao, S. (2020). Towards Automated 3D Inspection of Water Leakages in Shield Tunnel Linings Using Mobile Laser Scanning Data. *Sensors (Basel)* 20.
- Li, X.G., Yuan, D.J. (2012). Response of a double-decked metro tunnel to shield driving of twin closely under-crossing tunnels. *Tunn. Undergr. Space Technol.* 28, 18-30.
- Xu, G.W., He, C., Lu, D.Y., Wang, S.M. (2019). The influence of longitudinal crack on mechanical behavior of shield tunnel lining in soft-hard composite strata. *Thin-Walled Struct.* 144, 23.
- Chen, J.S., Mo, H.H. (2009). Numerical study on crack problems in segments of shield tunnel using finite element method. *Tunnelling and Underground Space Technology* 24, 91-102.
- Huang, H.W., Shi, J.K., Wang, F., Zhang, D.M., Zhang, D.M. (2020b). Theoretical and Experimental Studies on the Signal Propagation in Soil for Wireless Underground Sensor Networks. *Sensors* 20, 17.
- Bennett, P.J., Soga, K., Wassell, I., Fidler, P., Abe, K., Kobayashi, Y., Vanicek, M. (2010b). Wireless sensor networks for underground railway applications: case studies in Prague and London. *Smart. Struct. Syst.* 6, 619-639.
- Yin, J.G., Huang, H.W. (2015). Real time monitoring method for the longitudinal settlement of shield tunnel using wireless inclinometer, in: Chen, Y.N., Zeng, X.Q. (Eds.), Proceedings of the 2015 Information Technology and Mechatronics Engineering Conference. *Atlantis Press, Paris*, pp. 274-280.
- Zhao, D.P., Fan, H.B., Jia, L.L. (2021). Characteristics and Mitigation Measures of Floor Heave in Operational High-Speed Railway Tunnels. *Ksce Journal of Civil Engineering* 25, 1479-1490.
- Wang, F.N., Yin, S.Y., Guo, A.P., Wang, Z.C., Mi, M., Qi, G., Ma, J., Zhang, H.J. (2021a). Frame Structure and Engineering Applications of the Multisource System Cloud Service Platform of Monitoring of the Soft Rock Tunnel. *Geofluids* 2021, 15.
- Huang, H.W., Zhang, D.M., Ayyub, B.M. (2017b). An integrated risk sensing system for geo-structural safety. *Journal of Rock Mechanics and Geotechnical Engineering* 9, 226-238.